EPJ Web of Conferences **67**, 02060 (2014)
DOI: 10.1051/epjconf/20146702060

Study of Temperature Fields at Sprinkled Smooth and Sandblasted Tube Bundle

Petr Kracík[1,a], Ladislav Šnajdárek[1] and Jiří Pospíšil[1]

[1]Institute of Power Engineering, Brno University of Technology, Faculty of Mechanical Engineering, Technická 2896/2, 616 69 Brno, The Czech Republic

Abstract. The paper focuses on the influence of sprinkled tube surface on distribution of temperature fields, i.e. the heat transfer coefficient on the tubes surface. Two types of tubes have been tested, a smooth one and a sandblasted one in particular. A tube bundle comprises of thirteen copper tubes divided into two rows and it is located in a low pressure chamber where vacuum is generated using an exhauster via ejector. The liquid tested was water at an absolute pressure in a chamber in between 97 kPa up to 10 kPa and a thermal gradient 55 to 30 °C. The flow of the falling film liquid ranged between zero and 17 litres per minute.

1 Introduction

At a horizontal tube bundle sprinkled by a liquid of a low flow rate, a thin liquid film is formed that facilitates effective heat transfer. As the liquid flows, the liquid phase is promptly separated from the vapour phase which increases the heat transfer coefficient. This technology is applied for instance at sea water distillation. This distillation principle is based on low temperatures that vary by tens of degrees Centigrate but it is necessary to adequately lower the pressure of the area in which a tube bundle is positioned to enable evaporation. The advantage of this method is that it can utilize low-potential waste heat of other power-producing processes.

The European countries and the USA emphasize saving the primary fuel entering power-producing processes. Apart from boosting efficiency of power-producing processes and lowering energy consumption it is also possible to use the waste heat for coolness production. There are two predominant technologies of coolness production. The first method utilizes compressor cooling devices which are, however, very heavy on electric power. Absorption circulation represents their feasible alternative. Although being larger and more expensive, it consumes approximately one fifth of the electric power. The basic element of a single-stage absorption circulation consists of two exchangers operating in a low-pressure environment – the absorber and the desorber. The heat carrying agent's steam is cooled in the absorber, absorbed into an absorbent; excess heat must be conducted away properly. In a simplified way, it is a sprinkled exchanger on the surface of which the water steam condensates. The primary heat is supplied to the cycle in desorber, so the heat is provided to the cooling liquid and water boils at tube surface. And it is the study of thermodynamic mechanisms from the perspective of sprinkle modes when supplying heat to a cooling liquid that this paper focuses on.

2 Sprinkle mode

A liquid flowing through a horizontal tube bundle may form three basic sprinkle modes visible in Figure 1. These are the Droplet mode (a), the Jet mode (b) and the Membrane (Sheet) mode (c). These three modes are hereinafter referred to as the "D", "J" and "S" modes.

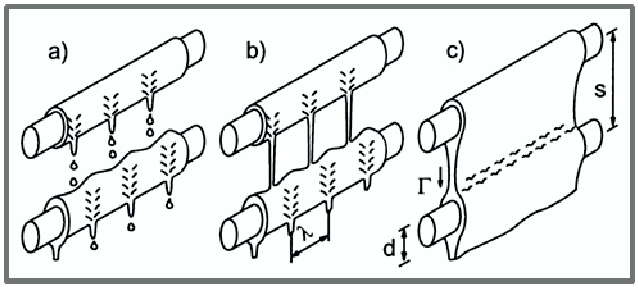

Figure 1 Sprinkle Modes [1]

With an increasing falling film liquid flow rate the transition from the Droplet to the Jet mode is defined by the formation of one stable column of liquid in among the droplets (this transition mode will be hereinafter referred to as the "D→J" mode). The transition from the Jet to the Membrane (Sheet) mode is defined by the connection of two columns and their formation of a small triangular sheet (hereinafter referred to as

[a] Corresponding author: kracik@fme.vutbr.cz

the "J→S" mode). In this mode, columns and leaves exist side by side. With a decreasing falling film liquid flow rate the reverse process takes place. That means that the formation of a stable liquid flow among the sheets is referred to as the Sheet-Column state (hereinafter referred to as the "S→J" mode) and the disintegration of the first column in the Column mode and its replacement by droplets changes the state to the Jet-Droplet mode (hereinafter referred to as the "J→D" mode). In case that the transition sprinkle mode is described without an arrow marking the direction of the falling film liquid increase/decrease but with a dash, then the change of the flow rate is not considered.

2.1 falling film liquid flow rate change

A particular sprinkle mode is influenced by a number of operational parameters. The first of them is the influence of a change in the falling film liquid flow rate increase/decrease on the distance between the droplet columns, i.e. the frequency of drops, described in a study conducted at the Victoria University (Australia) [4]. An experimental set was constructed at this university in order to verify the numerical model. It consisted of three identical cylinders positioned in a parallel way one below the other (three diameters were tested: 0.1 m, 0.05 m and 0.02 m). The sprinkle mode itself was recorded by a digital camera recorder. The Figure 2 illustrates the dependence of the drop frequency (i.e. the number of drops per second to fall onto the middle cylinder) and the dimensionless wavelength (i.e. the wavelength describing the distance between the droplet columns divided by surface tension, also referred to as capillary constant) on the Reynolds number.

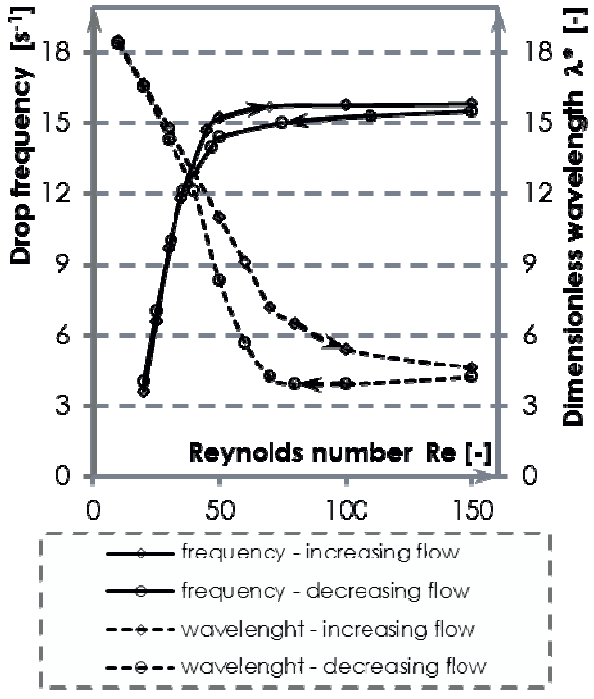

Figure 2 Dependence of drop frequency and dimensionless wavelength on the Reynolds number [4]

This Figure shows these two quantities for a monotonously increasing and decreasing flow rate. Measuring was conducted in the Reynolds number range of 20 – 150 [-] and it was discovered that the dependence of the frequency on the Reynolds number is very similar, however, when decreasing the flow rate the drops started to separate in a slightly slower pace in comparison with the increasing flow rate, which is visible particularly in the Reynolds number range of approx. 50 – 100 [-]. The reason for these slightly lower values of drops separation can be deducted from the dimensionless wavelength where at the decreasing flow rate the liquid at the middle cylinder tends to maintain the current state as long as possible, i.e. the distance between the droplet columns gets even shorter which naturally results in the lower number of drops. At the Reynolds number of approx. 70 [-] a turning point occurs where the flow rate is decreased to the extent that the distance between the droplet columns starts to increase rapidly, i.e. the drop frequency starts to decrease sharply.

The influence of the flow rate changes at various diameters of sprinkled tubes was also researched for instance by Hu and Jacobi [3]. To conduct their research they have created an aerodynamic tunnel of acrylate transparent plastic of the cross section dimensions 203.2 x 304.8 mm where the speed of air flow moving in the opposite direction to the falling film liquid flow ranged between 1.0 and 15.0 $m \cdot s^{-1}$. The tube bundle tested consisted of a distribution tube, a stabilization tube that was positioned 1.4 mm below the distribution tube, a tested tube, a landing tube and a collecting channel. There were apertures of 1.0 mm diameter drilled into the distribution tube at 1.5 mm spans along the length of 229 mm. The tube diameters tested were 9.5; 12.7; 15.9; 19.0 and 22.2 mm.

For the sprinkled tube bundle in a still atmosphere (flowing air speed in the tube surroundings comes close to zero) Hu and Jacobi [3] verified the convenience of dependence between the Reynolds number that describes a hydrodynamic flow mode and the Galilei number that describes the liquid flow resulting from gravitation, to define the transition of individual sprinkle modes. This dependence can be generally expressed in the form

$$Re = A \cdot (Ga)^B \qquad (1)$$

where both dimensionless criteria cover seven physical parameters altogether; i.e. the falling film liquid flow rate, the falling film liquid dynamic viscosity, the falling film liquid density, the falling film liquid surface tension, the sprinkled tube diameter, the gap between the sprinkled tubes and the gravitational acceleration.

In the still mode it was discovered that the transitions between the individual sprinkle modes vary with an increasing and decreasing flow rate and criterial equations were determined for these modes according to the equation (1) where the "A" and "B" constants are given in Table 1 together with a relative error for each equation

Figure 3 describes borders at increasing and decreasing falling film liquid flow rate according to

the mentioned equations at atmospheric pressure and water temperatures 30 °C and 55 °C, which corresponds on the basis of [9] to a modified Galilei number $Ga^{0.25} \approx 476$ and 751 [-].

Table 1 Coefficients for equation (1) to determine the flow mode according to Hu and Jacobi **[3]**

a) Increasing flow							
D → D-J		D-J → J		J → J-S		J-S→ S	
A	B	A	B	A	B	A	B
0.121	0.284	0.159	0.282	1.880	0.222	2.088	0.220
(8.5 %)		(6.6 %)		(4.3 %)		(4.2 %)	
b) Decreasing flow							
S → S-J		S-J→ J		J → J-D		J-D→ D	
A	B	A	B	A	B	A	B
1.004	0.250	1.064	0.244	0.057	0.321	0.045	0.321
(3.9 %)		(3.8 %)		(8.4 %)		(6.2 %)	

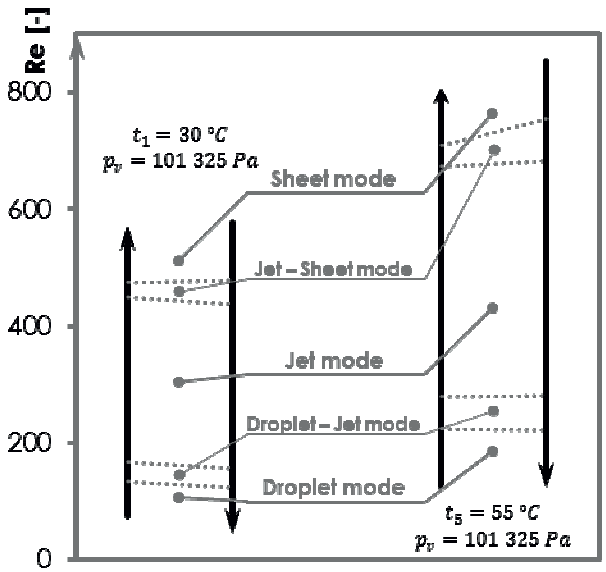

Figure 3 Sprinkle mode borders at increasing and decreasing flow rate according to Hu and Jacobi [3]

2.2 Influence of sprinkled tube diameter

In the study mentioned above [4] the cylinder diameter influence on the drop frequency and on the dimensionless wavelength in relation to the Reynolds number was researched, as displayed in Figure 4 for the lower (third) cylinder. The right horizontal axis stands for the drop frequency, i.e. how many drops have separated from the middle cylinder per second. The data presented in this Figure have only been obtained by measuring and they have not been compared with a numerical model. The 0.1 m, 0.05 m and 0.02 m diameters were studied and they are marked in the diagram legend as "freq. – exp. D = …". The measured values demonstrate a significant mode stability after the Reynolds number value 100 [-] has been reached. However, the increase preceding this value has been relatively steady despite the fact that it amounts to approx. 24% at 0.02 m diameter, approx. 44% at the 0.05 m diameter and 38% at the largest 0.1 m diameter. The authors do not state the span and surface type of cylinders.

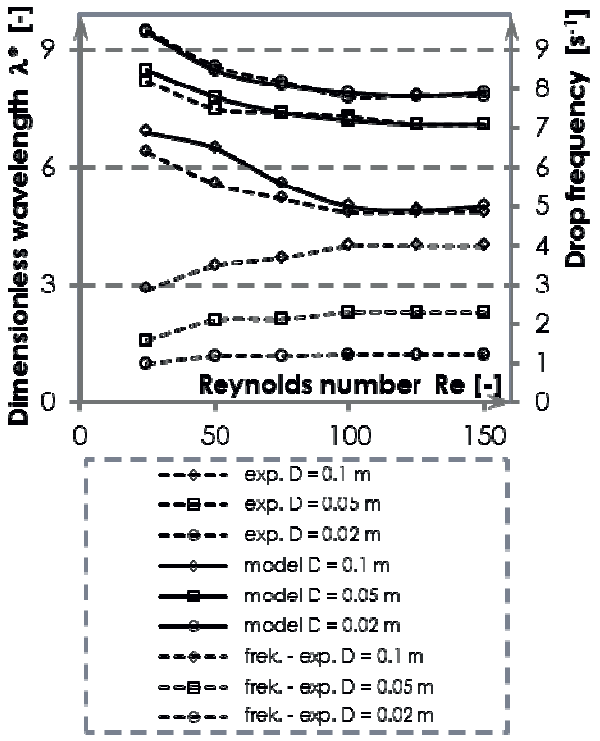

Figure 4 Influence of cylinder diameter on drop frequency and dimensionless wavelength [4]

The upper half of the Figure 4 illustrates the dependences of the dimensionless wavelength on the Reynolds number for all three studied diameters. The results of the experiment (marked in the legend as "exp. D = ...") and of the numerical model (marked in the legend as "model D = ...") are compared for each diameter. The authors found out that the difference of results between the experiment and the numerical model got smaller with a decreasing diameter. The authors give the deviation ranging between 1% and 2% at the smallest diameter, between 1.0% and 4.5% at the middle diameter and between 1.0% and 13.7% at the largest diameter. The final stability for the Reynolds number value 100 [-] achievement that occurred at these borders as well as at the drop frequency proves notable, although the stability at this quantity has been much more significant.

2.3 Influence of sprinkled tubes span

The influence of the gap between the sprinkled profiles on the flow mode type was tested by Wang et al. **[8]**. The bundle tested comprised of a distribution tube out of which a liquid was flowing (the substances tested were ethylene glycol and water), a tube of circular cross-section the purpose of which was to regulate the falling film liquid distribution and two flat tubes that created

a gap that demonstrated the flow mode. The flat tubes tested were made of a polished aluminium of the dimensions 400 x 25.4 x 3.18 mm (length x height x width). The measuring itself was preceded by a 2 to 3 hour tube sprinkling in order to ensure an ideal adherence of liquid to the surface (so that the surface was ideally wettable). The measurement procedure was followed to decrease the flow rate from the maximum and after the zero flow rate had been reached, it was again increased to the maximum possible rate. The measurement was repeated three times for each profile gap and only after these results were obtained the Reynolds numbers for the given mode transition and the relative error of these values were determined.

Table 2 Reynolds numbers for various tube pitches according to Wang et al. [8]

a) Increasing flow				
s-D [mm]	D → D-J	D-J → J	J → J-S	J-S → S
4.8	203	259	363	395
6.4	231	293	390	427
9.5	230	298	430	459
14.5	244	320	435	473
19.4	262	336	434	481
24.5	268	348	448	512
RMS%	4.21	1.40	0.84	2.34
b) Decreasing flow				
s-D [mm]	S → S-J	S-J → J	J → J-D	J-D → D
4.8	395	365	268	209
6.4	429	389	289	230
9.5	461	427	297	227
14.5	470	426	328	236
19.4	486	431	335	262
24.5	513	449	341	264
RMS%	0.87	0.77	1.53	4.53

Table 2 provides an overview of the measurement results where water of approximately the same physical properties that were expressed by the authors by means of the modified Galilei number $Ga^{0.25} \approx 450$ [-] was used as the falling film liquid. This value at atmospheric pressure (101 325 Pa) corresponds with the water temperature of approx. 27.4 °C (found in [9]).

To achieve the given measurement results, the authors set the gap between the stabilization tube and the first profile to 2.0 mm. Their results suggest that the larger the gap between the sprinkled profiles, the higher the Reynolds number for the given sprinkle mode. This increase, however, did not prove to be steady, i.e. in one case of the gap increase the next Reynolds number was even lower by approx. 1.0% which does not seem to be a correct value as the increasing gap causes the horizontal sprinkled diameter to increase as well and therefore more liquid, i.e. higher flow rate, is necessary at a larger gap in order to achieve the same sprinkle mode. When comparing the Reynolds numbers belonging to the smallest and the largest gaps between the profiles at individual modes the increase ranges between approx. 23% and 32%. The difference of the Reynolds numbers between the increasing and decreasing flow rate at individual states equals on average 1.1% with a standard deviation of 1.1%.

2.4 Comprehensive determination of sprinkle mode areas

In the above mentioned study by Hu and Jacobi [3] the conclusion was reached on the basis of the measurement that neither the diameter of sprinkled tubes nor the gap between them exercises any significant influence on a sprinkle mode. The tested ratio of the gap between tubes and the sprinkled tube diameter ranged approx. from 0.22 to 5.3 [-]. For the purposes of practical application and comparison with other authors equations for individual modes were created without distinguishing the increase or decrease of the falling film liquid flow rate, while the relative error did not significantly increase. Constants for individual equations derived from the equation (1) are given in Table 3, i.e. they are displayed in Figure 5 in the Reynolds number and the modified Galilei number range 0 to 600 [-].

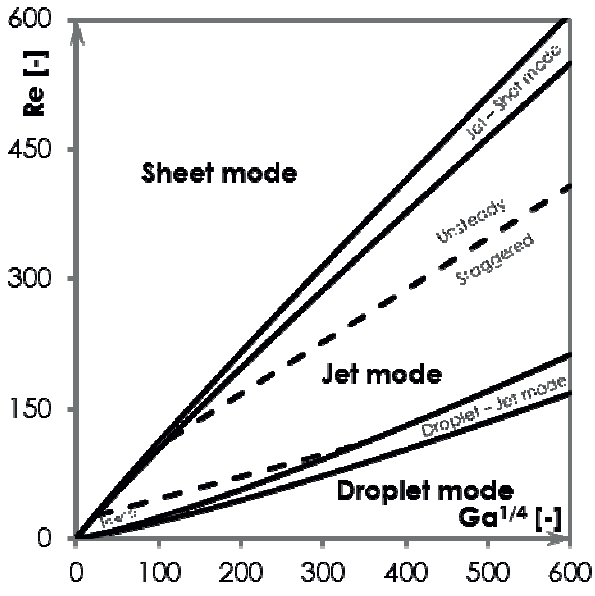

Figure 5 Sprinkle modes borders according to Hu and Jacobi [3]

Figure 5 also illustrates three Jet mode types that Hu and Jacobi specified. The first one is a so called "in-line" Jet mode type. This mode type occurs at low falling film liquid flow rates and the liquid falls down in columns that are connected in front of the tube and behind it. I.e. they create a single row and they do not move vertically. The border of this mode is determined by the equation (2) that does not distinguish the increase

or decrease of the flow rate and the relative error of the equation is 12.5%.

$$Re = 20.53 + 0.256 \cdot (Ga)^{0.25} \quad (2)$$

The other two phases of the Jet mode are states where in the first case the columns pendulate vertically around an imaginary point and in the second case the way columns move can no longer be predicted. The border between these phases is determined for increasing and decreasing falling film liquid flow rate in the equation (3), where the relative error of the equation is set at 8.3%.

$$Re = 47.42 + 0.600 \cdot (Ga)^{0.25} \quad (2)$$

Other authors who dealt with experimental division of sprinkle modes are Armbruster and Mitrovic who published the results of their research for instance in **[2]**. Their experimental device consisted of a distribution vessel of 260 mm length with apertures of 1 mm diameter at 3 mm span at the bottom, a stabilization tube of 18 mm diameter positioned directly below the apertures, a test tube (also of 18 mm diameter) and a collection drain. The liquid tested was distilled water in temperature range from 15 to 55 °C. The mass flow of water ranged between 0.02 and 0.24 kg/(s·m) and it was determined by a differential method, i.e. by weighing the distribution vessel both before and after the particular mode testing. From the values measured for individual borders the functional dependence was set according to the equation (1) and the final constants are given in Table 3. However, no relative error is mentioned at their equations.

Table 3 Reynolds numbers for various tube pitches according to Wang et al. [8]

		Armbruster and Mitrovic [2]	Hu and Jacobi [3]		Roques et al. [7]
D – D-J	A	0.200 0	0.074	(11.0 %)	0.041 7
	B	0.250 0	0.302		0.327 8
D-J – J	A	0.260 0	0.096	(11.2 %)	0.068 3
	B	0.250 0	0.301		0.320 4
J – J-S	A	0.920 0	1.414	(5.8 %)	0.855 3
	B	0.250 0	0.233		0.248 3
J-S – S	A	1.140 0	1.448	(6.6 %)	1.068 0
	B	0.250 0	0.236		0.256 3

Table 3 also shows the results of Roques et al. [7]. In order to determine sprinkle modes they created an experimental device consisting of a distribution vessel with a flat bottom of 260 x 10 mm and drilled apertures of 1.0 mm diameter at 2.0 mm span along the length of 200 mm. There were three tested copper tubes of 19.04 mm positioned below the bottom that have been sandblasted before the testing itself and thus hollows of approx. 0.3 μm to 2.0 μm were formed at their surface.

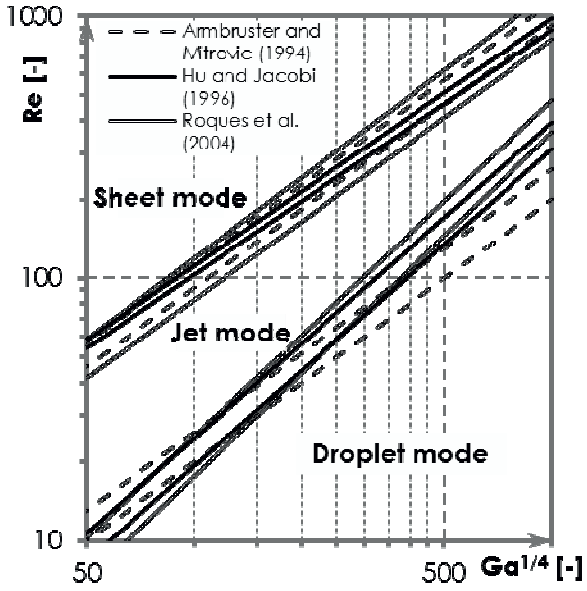

Figure 6 Comparison of sprinkle modes' borders by various authors

Figure 6 presents a comparison of individual sprinkle modes' borders described by the above mentioned authors and the constants determined by them given in Table 3 into the equation (1). Values in the diagram are displayed in a logarithmic scale; i.e. the Reynolds number in the range from 10 to 1 000 [-] and the modified Galilei number in the range from 50 to 1 000 [-]. The diagram clearly shows a certain correspondence of the trend between the Jet and the Sheet mode, but in the case of a transition from the Jet to the Droplet mode it is not so evident. The narrowest transition strips are in the case of Hu and Jacobi, which is 30% to 60% compared to Armbruster and Mitrovic, but their data were obtained at a smaller experimental sample.

3 Experimental device

For the purpose of heat transfer at sprinkled tube bundles research an experimental device has been constructed consisting of a cylinder vessel of 1.2 m length with a tube bundle positioned inside. Vacuum is generated in the chamber using an exhauster via ejector. Tube bundle with a geometry visible in Figure 7 consists of copper tubes of 12 mm outer diameter.

Two geometrically identical tube bundles differentiated by a sprinkled tube surface were studied. The first bundle consisted of smooth tubes and the second one of sandblasted tubes. The difference between the individual surface types is visible in Figure 8.

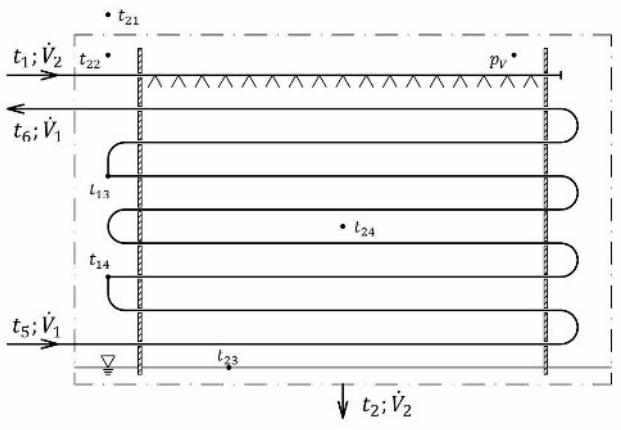

Figure 7 Simplified diagram of tube bundle

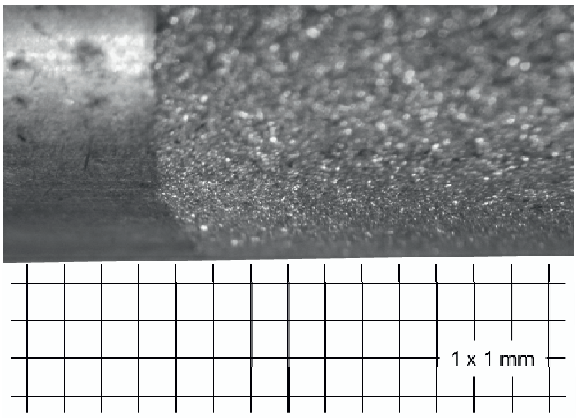

Figure 8 Sprinkled tube surface types (smooth one on the left and sandblasted one on the right)

Further details on the experimental device are published for instance at [5, 6] including partial measurement results.

The calculation of the heat transfer coefficient in this paper is based on the thermal balance according to the law of conservation of energy based on a simplified diagram in Figure 7, the Newton's law of heat transfer and the Fourier's law of heat conduction.

4 Measurement results

The experiments described in this paper involved the heating of a falling film liquid. That means that hot water of the average input temperature 55.2 °C and the average flow rate 12.4 l·min was flowing inside smooth tubes^{-1}. The average falling film liquid temperature at the distribution tube outlet was 29.9 °C and the tested falling film liquid flow rate ranged from 0 to 15.8 l·min^{-1}. In case of sandblasted tubes hot water of the average input temperature 55.1 °C and the average flow rate 13.7 l·min^{-1} was flowing and the exchanger was sprinkled by cold water of average temperature at the distribution tube outlet of 29.8 °C and the volumetric flow rate ranged between zero and 16.1 l·min^{-1}. Tested range of an absolute pressure in the chamber ranged in both cases from 12.3 kPa(a) to the atmospheric pressure that was at the time of measurement 96.8 kPa(a) on average.

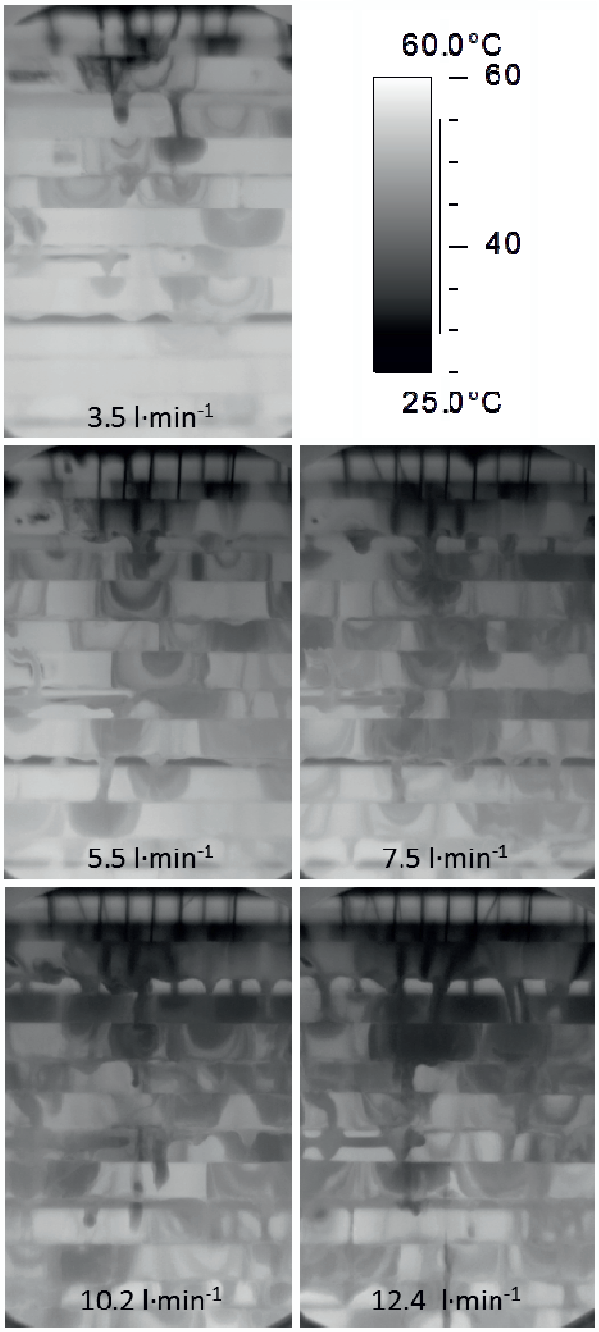

Figure 9 Images of thermographic measurement

Figure 8 shows images of thermographic measurement recorded by a thermographic camera FLIR SC 660 with the resolution of 640 x 480 pixels during the whole measuring process at smooth and sandblasted tubes. The scale of all images ranges between 25 – 60 °C and the exchanger gradient is the above mentioned 55 °C to 30 °C. The falling film liquid outlet from a distribution tube is visible at the upper part of the images. The first image was captured during the falling film liquid flow rate 3.5 l·min^{-1} and it is a pure Droplet mode. The second image records the flow rate of 5.5 l·min^{-1} and due to a sufficient amount of liquid first columns can be distinguished. This border was approximately the same in smooth and sandblasted tubes. The third and fourth image display the flow rate 7.5 and 10.2 l·min^{-1},

respectively. A gradual increase in the number of columns and a corresponding decrease of drops can be observed. In spite of this fact the Droplet mode dominates in the lower part of the bundle. The last image illustrates the flow rate 12.4 $l \cdot min^{-1}$ that is approximately the top border of the Droplet-Jet mode.

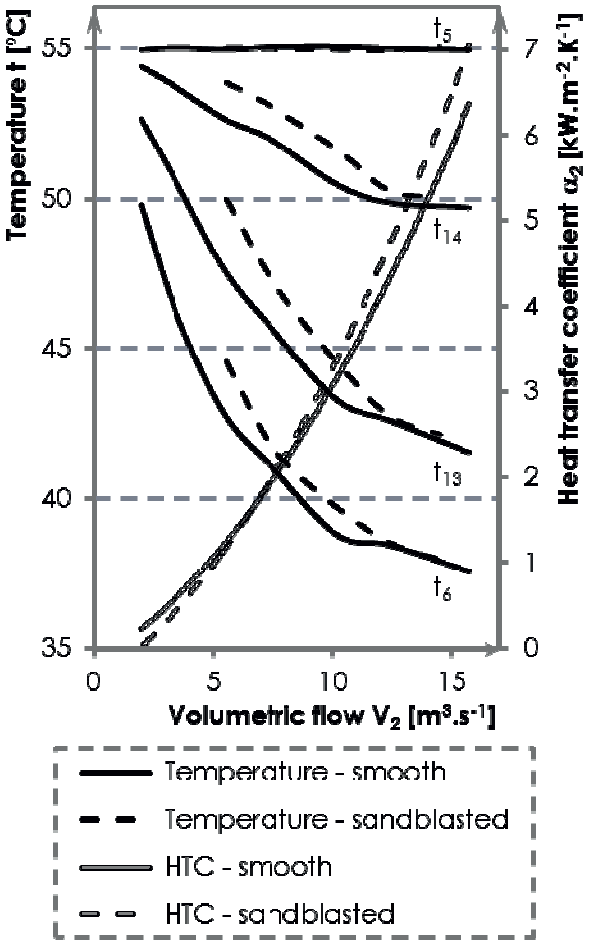

Figure 10 Waveforms of temperature in exchanger and of mean heat transfer coefficient at tube surface in relation to falling film water flow rate

Figure 10 depicts the cooling liquid temperature (the liquid flowing inside the tubes) in relation to the falling film liquid flow rate. The temperatures were measured at the beginning (t_5) and at the end of the bundle (t_6; the bundle's length is 12.22 m) and afterwards the temperatures were measured at 2.86 m (t_{13}) and 8.46 m (t_{15}; considered in the direction opposite to the cooling liquid flow) during the sprinkling process. Full curves represent the smooth-tube exchanger and the dashed curves illustrate the sandblasted-tube exchanger.

The same image also displays the waveforms of the studied transfer coefficient in smooth and sandblasted tubes with a relative error 4.3% ±4.3 in smooth tubes and 4.7% ±4.3 in sandblasted tubes. These waveforms were determined from the total number of 4 487 measured points.

5 Conclusions

The paper's objective was to briefly describe basic potential thermodynamic interconnections from the perspective of falling film liquid and basic physical parameters that exercise their influence on a sprinkle mode. There are various studies dealing with the basic sprinkle modes' phases and their transitions, however, no general consensus has been reached as to which parameters have a practical influence on a sprinkle mode. The research conducted at the Brno University of Technology, Energy Institute, dept. of Power Engineering aims to delineate these mechanisms. This paper presents the results that have been studied at two geometrically identical exchangers differentiated by a surface type; in particular a smooth one and a sandblasted one.

Due to the tube bundle size and the falling film liquid volumetric flow rate only the Jet mode (Staggered) has been reached at maximum flow rate. Based on a visual observation, the transitions corresponding best were those defined by Armbruster and Mitrovic (1994). In our case, however, there is a real bundle, not only three tubes positioned horizontally one below each other. The temperature in this bundle varies according to the height and therefore individual modes occur successively and it is difficult to determine one specific mode directly.

The main results of our research activity are presented in Figure 10. This Figure shows four temperatures measured inside the exchanger. As the temperature change clearly suggests, there is a smaller thermal gradient in sandblasted tubes in comparison to smooth ones at low flow rates and consequently this part also proves a lower heat transfer coefficient at tube surface. A possible reason for this can be an incomplete water wrapping of the sandblasted tube surface due to its roughness. However, the flow rate increase makes this difference diminish. This can be caused by an already existing complex stabilized water film that the main stream slides along and that is thicker than in smooth tube.

Our further research will focus on other types of tube surfaces and their influence on the heat transfer coefficient and various admixtures both soluble and insoluble in water which affect the surface tension at decreasing pressure and we would like to identify the advantage of low pressure inside a chamber as the heat transfer coefficient reacts differently with some flow rates at tube bundle than a coefficient measured at one, two or three tubes placed horizontally one above the other.

Acknowledgement

This paper was created with the financial support of the Czech Science Foundation within the P101/10/1669 grant and the NETME Centre project funded by the Operational Programme Research and Development for Innovations that is co-funded by ERDF (European Regional Development Fund).

References

1. Armbruster, R. J. Mitrovic, Experimental Thermal and Fluid Science **18** (3), 183 (1998)
2. Armbruster, R. J. Mitrovic, *Proceedings of the 10th international heat transfer conference* **3**, 275 (1994)
3. Hu, X. A. M. Jacobi, Journal of Heat Transfer **118** (3), 616 (1996)
4. Jafar, Thorpe and Turan, *Computational fluid dynamics seventh international conference on CFD in the minerals and process industries*. (2009)
5. P. Kracík, J. Pospíšil, L. Šnajdárek, Acta Polytechnica **52** (3), 48 (2012)
6. P. Kracík, L. Šnajdárek, J. Pospíšil, EPJ Web of Conferences **45** (01052), (2013)
7. J.F. Roques, V. Dupont and J. R. Thome. Journal of Heat Transfer [online] **124** (3), 491 (2002)
8. X. Wang, P. S. Hrnjak, S. Elbel, A. M. Jacobi and M. He, Journal of Heat Transfer **124** (2), 1 (2012)
8. X-ENG. X Steam Tables for MS Excel [počítačový soubor .xls]. Ver. 2.6. [online]. [cit. 30.11.2010]. Freeware. <http://www.x-eng.com/XSteam_Excel.htm>.

Nomenclature

A, B [-]	constants in the equatin (1)
α [$W \cdot m^{-2} \cdot K^{-1}$]	heat transfer coefficient
D [m]	diameter
D	droplet mode
D-J	droplet – jet mode
exp.	experiment
freq.	frequncy
Ga [-]	Galileo number
J	jet mode
J-D	jet – droplet mode
J-S	jet – sheet mode
p [Pa]	pressure
Re [-]	Reynolds number
S	sheet mode
S-J	sheet – jet mode
t [°C]	temperature
V [$m^3 \cdot s^{-1}$]	volumetric flow

Subscripts

1 condition of falling film liquid in distribution tube
2 condition of falling film liquid at vessel bottom
5 condition of the cooling/heating liquid at loop input
6 condition of the cooling/heating liquid at loop output
o condition outside the tube
V vacuum loop